HHS Public Access

Author manuscript

Kidney Int. Author manuscript; available in PMC 2023 November 01.

Published in final edited form as:

Kidney Int. 2022 November ; 102(5): 1030–1041. doi:10.1016/j.kint.2022.06.027.

Multiple molecular mechanisms are involved in the activation of the kidney sodium-chloride cotransporter by hypokalemia

Adrián R. Murillo-de-Ozores, PhD[1,2], **Héctor Carbajal-Contreras, MD**[1,3], **Germán R. Magaña-Ávila, MD**[1,2], **Raquel Valdés, BS**[1,4], **Leoneli I. Grajeda-Medina, MD**[1], **Norma Vázquez, BS**[4], **Teresa Zariñán, PhD**[5], **Alejandro López-Saavedra, PhD**[6], **Avika Sharma, BS**[7], **Dao-Hong Lin, PhD**[8], **Wen-Hui Wang, MD**[8], **Eric Delpire, PhD**[9], **David H. Ellison, MD**[7,10,11], **Gerardo Gamba, MD PhD**[1,3,4], **María Castañeda-Bueno, PhD**[*,1]

[1]Department of Nephrology and Mineral Metabolism, Instituto Nacional de Ciencias Médicas y Nutrición Salvador Zubirán, Tlalpan, Mexico City

[2]Facultad de Medicina, Universidad Nacional Autónoma de México, Coyoacan, Mexico City

[3]PECEM (MD/PhD), Facultad de Medicina, Universidad Nacional Autónoma de México, Coyoacan, Mexico City, Mexico

[4]Molecular Physiology Unit, Instituto de Investigaciones Biomédicas, Universidad Nacional Autónoma de México, Tlalpan, Mexico City.

[5]Red de Apoyo a la Investigación (RAI), Universidad Nacional Autónoma de México (UNAM) - Instituto Nacional de Ciencias Médicas y Nutrición Salvador Zubirán (INCMNSZ), Mexico City, Mexico

[6]Unidad de Aplicaciones Avanzadas en Microscopía del Instituto Nacional de Cancerología y la Red de Apoyo a la Investigación, Universidad Nacional Autónoma de México, Mexico City, Mexico

[7]Division of Nephrology and Hypertension, Department of Medicine, Oregon Health and Science University, Portland, OR, USA

[8]Department of Pharmacology, New York Medical College, Valhalla, NY, USA

[9]Department of Anesthesiology, Vanderbilt University School of Medicine, Nashville, TN, USA;

[10]Oregon Clinical & Translational Research Institute, Oregon Health & Science University, Portland, OR, USA;

[11]Renal Section, VA Portland Health Care System, Portland, OR, USA.

Abstract

Low potassium intake activates the kidney sodium-chloride cotransporter, NCC, whose phosphorylation and activity depend on the With-No-Lysine kinase 4 (WNK4) that is inhibited

[*]**Correspondence:** María Castañeda-Bueno, PhD, maria.castanedab@incmnsz.mx, mcasta85@yahoo.com.mx, Av. Vasco de Quiroga 15. Col. Secc. XVI-Belisario Dominguez. Tlalpan, 14080, CDMX, Mexico.

DISCLOSURE

All authors declared no competing interests.

SUPPLEMENTARY MATERIAL

Supplementary information is available on Kidney International's website.

by chloride binding to its kinase domain. Low extracellular potassium activates NCC by decreasing intracellular chloride thereby promoting chloride dissociation from WNK4 where residue L319 of WNK4 participates in chloride coordination. Since the WNK4-L319F mutant is constitutively active and chloride-insensitive *in vitro*, we generated mice harboring this mutation that displayed slightly increased phosphorylated NCC and mild hyperkalemia when on a 129/sv genetic background. On a low potassium diet, upregulation of phosphorylated NCC was observed, suggesting that in addition to chloride sensing by WNK4, other mechanisms participate which may include modulation of WNK4 activity and degradation by phosphorylation of the RRxS motif in regulatory domains present in WNK4 and KLHL3, respectively. Increased levels of WNK4 and kidney-specific WNK1 and phospho-WNK4-RRxS were observed in wild type and $WNK4^{L319F/L319F}$ mice on a low potassium diet. Decreased extracellular potassium promoted WNK4-RRxS phosphorylation *in vitro* and *ex vivo* as well. These effects might be secondary to intracellular chloride depletion, as reduction of intracellular chloride in HEK293 cells increased phospho-WNK4-RRxS. Phospho-WNK4-RRxS levels were increased in mice lacking the Kir5.1 potassium channel, which presumably have decreased distal convoluted tubule intracellular chloride. Similarly, phospho-KLHL3 was modulated by changes in intracellular chloride in HEK293 cells. Thus, our data suggest that multiple chloride-regulated mechanisms are responsible for NCC upregulation by low extracellular potassium.

Keywords

distal convoluted tubule; potassium; blood pressure; epithelial transport; Familial Hyperkalemic Hypertension; Gitelman syndrome

INTRODUCTION

Studies have revealed an inverse correlation between K^+ consumption and blood pressure levels in humans[1–3]. Lower K^+ consumption has been linked to higher blood pressure[1] and higher risk of cardiovascular events[4]. These effects are probably secondary to kidney Na^+ retention under low K^+ intake, given the central role of the kidneys for the long term regulation of blood pressure[5]. In mice, dietary K^+ restriction causes a salt-sensitive increase in blood pressure[6,7], that is not observed in mice deficient in the thiazide-sensitive NaCl cotransporter (NCC), suggesting NCC involvement in this phenomenon[7].

NCC constitutes the major Na^+ pathway in the apical membrane of the distal convoluted tubule (DCT). The DCT reabsorbs 5–10% of the filtered Na^+, whereas no net K^+ reabsorption or secretion occur within this segment[8]. Nevertheless, NCC activity influences kidney K^+ excretion by negatively affecting the activity of the K^+ secretory apparatus that operates in more downstream segments[9]. Thus, loss of function mutations in the gene encoding NCC (*SLC12A3*)[10] cause Gitelman syndrome that presents with hypokalemia, whereas Familial Hyperkalemic Hypertension is primarily driven by overactivation of NCC[11,12] and is caused by mutations in genes that regulate NCC function, such as *WNK1, WNK4*[13], *KLHL3,* and *CUL3*[14,15].

NCC activity is positively regulated by phosphorylation in several sites within its amino-terminal domain[16], by the STE20/SPS1-related Proline-Alanine-rich Kinase (SPAK) and the

Oxidative Stress-Responsive 1 kinase (OSR1)[17]. Both kinases are substrates of the With-No-Lysine (K) (WNK) family of kinases[18]. Although this family comprises 4 members, WNK4 is the major regulator of NCC[19,20] and participates in its activation by different stimuli[21].

NCC activity is highly sensitive to subtle changes in extracellular K^+ concentration ($[K^+]_e$)[22–24]. Basolateral Kir4.1/Kir5.1 heterotetrameric K^+ channels in the DCT have been proposed as the "potassium sensor" because small decreases in $[K^+]_e$ promote K^+ exit through these channels, and thus hyperpolarization of the basolateral membrane, whereas increases in $[K^+]_e$ cause depolarization[25,26]. These changes in cell membrane potential affect the driving force for basolateral Cl^- efflux, mainly through the ClC-Kb channels[27]. Thus, lower $[K^+]_e$ promotes hyperpolarization, increases Cl^- efflux, and reduces intracellular Cl^- concentration ($[Cl^-]_i$). The activity of WNK4 has been shown to be highly sensitive to $[Cl^-]$[28,29] given that a Cl^- ion can bind to the active site of the enzyme that stabilizes an inactive conformation, preventing autophosphorylation and activation [28,30]. Thus, in the setting of low $[K^+]_e$, the reduction in $[Cl^-]_i$ promotes Cl^- dissociation and activation of the WNK4-SPAK/OSR1-NCC pathway.

An additional mechanism for low $[K^+]_e$-mediated activation of the WNK4-SPAK/OSR1-NCC pathway has been proposed[31] that involves modulation of the activity of the CUL3-KLHL3 E3 complex that regulates WNK4 ubiquitylation and degradation[32,33]. In mice, reduction of dietary K^+ promoted an increase in KLHL3 phosphorylation at a Protein Kinase C (PKC)/Protein Kinase A (PKA) consensus motif (RRxS) within the substrate binding domain of the protein. Previously, it was shown that this phosphorylation prevents KLHL3-targeted degradation of WNK4 in cultured cells[34]. Accordingly, higher kidney WNK4 levels were observed in mice on low K^+ diet (LKD).

Finally, in addition to regulation by Cl^- binding, WNK4 catalytic activity can be regulated by phosphorylation of sites located within the regulatory N- and C-terminal domains (Ser64 and Ser1196, here referred to as RRxS sites in allusion to the sequence that encompasses the phosphorylated residue)[35]. In vitro and in cultured cells, PKA and PKC can phosphorylate these sites. Phosphoablative mutations drastically reduce kinase activity even in the context of impaired Cl^- binding, and phosphorylation of these sites is necessary to achieve maximal activation of the Cl^--insensitive mutant (L319F)[35].

For the present work we generated a mouse model that carries a mutation in the WNK4 Cl^- binding site (L319F) that renders the kinase constitutively active and insensitive to inhibition by Cl^- as suggested by in vitro data.[28,35] We used this model to assess the role of direct Cl^- binding to WNK4 for the modulation of the WNK4-SPAK/OSR1-NCC pathway in response to low $[K^+]_e$ *in vivo*. Interestingly, we observed that $WNK4^{L319F/L319F}$ mice can still upregulate NCC phosphorylation in response to an LKD. Thus, additional mechanisms may participate in this regulation that we begin to characterize and that may involve WNK4 and KLHL3 phosphorylation at RRxS sites.

METHODS

Mice studies

Animal studies were approved by the animal care and use committee of Instituto Nacional de Ciencias Médicas y Nutrición Salvador Zubirán. An LKD (0% K^+) or normal K^+ (1.2% K^+) diet was given for 7 days before mice were killed. Blood and kidneys were harvested for molecular and biochemical analysis. For more details refer to Supplementary Methods.

Western Blot

Protein concentration of tissue or cell lysates was determined by the BCA protein assay (Pierce). Laemmli buffer was added to protein extracts before heating to 95°C for 5 minutes. Samples were subjected to sodium dodecylsulfate-polyacrylamide gel electrophoresis and transferred to polyvinylidene difluoride membranes. Membranes were blocked for 1 hour in 10% (w/v) nonfat milk in triethanolamine-buffered saline with 0.1% Tween 20 (TBST). Antibodies were diluted in TBST containing 5% (w/v) nonfat milk. Membranes were incubated with primary antibodies overnight at 4°C and with horseradish peroxidase-coupled secondary antibodies at room temperature for 1 hour. Signals were detected with enhanced chemiluminescence reagent.

Immunofluorescence

Mice were anesthetized with isoflurane and perfused with 20 ml of phosphate-buffered saline and then with 20 ml of 4 % (w/v) paraformaldehyde in phosphate-buffered saline. Harvested kidneys were incubated for 3 hours in 4 % paraformaldehyde and then overnight in 30 % (w/v) sucrose in phosphate-buffered saline at 4°C. Tissues were then mounted in OCT (Tissue-Tek) and 5-μm sections were cut and stored at −80°C. For immunostaining, sections were washed with TBST. Blocking was performed with 10 % (w/v) bovine serum albumin diluted in TBST for 30 minutes at room temperature, before incubation with primary and secondary antibodies. Antibodies were diluted in in TBST with 5% (w/v) bovine serum albumin. Imaging was performed using a LSM710-DUO confocal microscope (Carl Zeiss, Jena, Germany).

Antibodies

See Supplementary Table S1.

Cells

HEK293 cells (ATCC CRL-1573) were transiently transfected with mWNK4-HA[35] or hKLHL3-FLAG[34]. Cells were grown to 70–80 % confluence and transfected with Lipofectamine 2000 (Life Technologies). Forty-eight hours later, cells were lysed with a lysis buffer containing 50 mM Tris-HCl (pH 7.5), 1 mM ethyleneglycol-bis-(b-aminoethylether)-N,N,N0,N0-tetra-acetic acid, 1 mM ethylenediamine tetra-acetic acid, 50 mM sodium fluoride, 5 mM sodium pyrophosphate, 1 mM sodium orthovanadate, 1% (w/v) IGEPAL® CA-630 (Sigma), 270 mM sucrose, 0.1% (v/v) 2-mercaptoethanol, and protease inhibitors (complete tablets, 10 mM 1,10-phenanthroline, and 1 mg/ml pepstatin; Roche).

Modified media and small molecules used in HEK293 cells

Cells were incubated with different media for 16 hours before cell lysis to assess the effect of $[K^+]_e$ concentration. Media used were: low K^+ media (LKM; 135 mM NaCl, 1 mM KCl, 0.5 mM $CaCl_2$, 0.5 mM $MgCl_2$, 0.5 mM Na_2HPO_4, 0.5 mM Na_2SO_4, 15 mM HEPES, 27.75 mM glucose, 18 mM sucrose, pH 7.4); normal K^+ media (NKM; same as LKM except for 5 mM KCl and 10 mM sucrose to adjust osmolarity), or high K^+ media (HKM; same as LKM except for 10 mM KCl and no sucrose). The effect of $[Cl^-]_i$ depletion was assessed by incubating cells for 2 hours with a hypotonic low Cl^- media with normal K^+ (67.5 mM Na-gluconate, 5 mM K-gluconate, 0.5 mM $CaCl_2$, 0.5 mM $MgCl_2$, 0.5 mM Na_2HPO_4, 0.5 mM Na_2SO_4, 7.5 mM HEPES, 27.75 mM glucose, pH 7.4; modified from Vitari et al.[18]). In the indicated experiments, cells were preincubated with the WNK kinase inhibitor WNK463 (10 μM, gift from Dario Alessi) for 15 minutes before and during the maneuver (incubation in media with different K^+ content or hypotonic low Cl^-). Stimulation with N-ethylmaleimide (NEM; 100 μM, Sigma) was performed for 30 minutes before cell lysis.

Ex vivo kidney slices

Twelve-to 16-week-old male C57BL/6 mice were anesthetized with isoflurane and perfused with 20 m of a modified Ringer media with high K^+ (93.5 mM NaCl; 25 mM $NaHCO_3$; 10 mM KCl; 1mM NaH_2PO_4; 2.5 mM $CaCl_2$; 1.8 mM $MgCl_2$; 25 mM glucose). Kidneys were collected and placed in the same solution. Then, 250 μm slices were cut using a vibratome (PELCO easiSlicer). Slices were incubated at 30.5°C for 30 minutes in the same solution and then switched for another 60 minutes to control Ringer media (98.5 mM NaCl; 25 mM $NaHCO_3$; 5 mM KCl; 1mM NaH_2PO_4; 2.5 mM $CaCl_2$; 1.8 mM $MgCl_2$; 25 mM glucose) or to low K^+ Ringer media (the same as control except for 102.5 mM NaCl and 1 mM KCl). At the end of the experiment, slices were frozen with liquid N_2 and later homogenized as described above for whole mouse kidneys.

Statistical analysis

All values are expressed as mean ± SEM. For comparison between 2 groups, unpaired Student's t-test (2-tailed) was used. For comparison between multiple groups, analysis of variance test was performed, followed by Dunett post hoc tests. A difference was considered significant when $P < 0.05$.

RESULTS

$WNK4^{L319F/L319F}$ mice can still upregulate NCC phosphorylation in response to an LKD, suggesting that alternative pathways may participate.

The L319F mutation in mWNK4 (L322F in hWNK4) prevents Cl^- binding and promotes constitutive activation of the kinase[35,36]. We generated a mouse model carrying this mutation to assess its physiological consequences, as well as the ability of these mice to respond to dietary K^+ restriction (Supplementary Figure S1). $WNK4^{L319F/L319F}$ mice (C57Bl/6J background) presented higher NCC and pNCC levels (Figure 1). Although no significant electrolytic alterations were observed, there was a tendency toward higher plasma $[K^+]$ (Table 1). Of note, when evaluated in a different genetic background

(mixed B6–129/SV), higher pNCC, pSPAK/OSR1, and plasma [K^+] levels were observed (Supplementary Figure S2). For the rest of the study, mice on C57BL/6J background were used. Interestingly, upregulation of pNCC, NCC, and pSPAK/OSR1 in response to LKD was observed in both wild type and WNK4$^{L319F/L319F}$ mice, suggesting that the relief of WNK4 inhibition by Cl^- is not the only mechanism behind NCC activation in response to reductions in $[K^+]_e$ (Figure 2). Thus, additional mechanisms participate in this regulation that remain to be described.

WNK4 phosphorylation at S64 and S1196 increases in kidneys of mice on an LKD

Given that WNK4 is necessary for NCC activation by low K^+ intake[24,37] and that phosphorylation of its RRxS motifs is essential for full kinase activation, we decided to investigate if WNK4 phosphorylation at these motifs is modulated by LKD.

In kidneys of mice placed on a LKD for 7 days, in addition to the expected increases in WNK4, NCC, and pNCC (Figure 3a and b), the radio of pS64 and pS1196/total WNK4 increased, suggesting that the increase in phosphorylation was not solely the consequence of increased protein expression.

In the DCTs of mice on normal K^+ diet, a very low or undetectable signal was observed with the WNK4, pWNK4-S64, and pWNK4-S1196 antibodies by immunofluorescent staining (Figure 3c–h). In contrast, WNK bodies[38] were observed in DCT cells of mice on an LKD with all three antibodies. Thus, WNK bodies that are formed in DCT cells in response to an LKD[38,39] contain phosphorylated WNK4 at RRxS sites.

Finally, increased WNK4 and KS-WNK1 protein levels, as well as WNK4 phosphorylation levels at S64 and S1196 were observed with an LKD in WNK4$^{L319F/L319F}$ mice (Figure 4). Thus, modulation of WNK4 activity by phosphorylation of RRxS sites may contribute to upregulation of NCC activity under LKD.

Low $[K^+]_e$ and intracellular Cl^- depletion promote WNK4 phosphorylation at S64 and S1196 in HEK293 cells.

To test whether changes in $[K^+]_e$ can directly modulate WNK4-RRxS phosphorylation, we used WNK4-transfected HEK293 cells. Phosphorylation at S64 and S1196 increased after incubation of cells on an LKM, but did not decrease after incubation on a high K^+ medium (Figure 5a and b). Terker et al. showed that incubation of these cells in LKM decreased $[Cl^-]_i$[7]. Thus, we tested whether the increase in WNK4-RRxS phosphorylation could be stimulated by a reduction in $[Cl^-]_i$. Incubation in hypotonic low Cl^- medium[16,40] for 2 hours increased pWNK4-S64 and pWNK4-S1196 (Figure 5c and d). As an alternative maneuver to reduce $[Cl^-]_i$, we used N-ethylmaleimide (NEM). NEM is a known activator of K^+:Cl^- cotransporters (KCCs) and inhibitor of Na^+-dependent Cl^- cotransporters (N(K)CCs),[41] which is known to reduce $[Cl^-]_i$ [42]. The addition of NEM also increased pWNK4-S1196 (Figure 5e and f) and pWNK4-S64 levels (Supplementary Figure S3A).

Reasoning that WNK4-RRxS phosphorylation under LKM could be mediated, directly or indirectly, by increased WNK activity under low $[Cl^-]_i$, we tested whether the specific WNK inhibitor WNK463[43] could prevent it. Surprisingly, WNK463 increased WNK4

abundance and WNK4 phosphorylation at S64 and S1196, regardless of the $[K^+]_e$ (Figure 5g and h, Supplementary Figure S3B). Like NEM[42], WNK463 decreases endogenous SPAK activity, and thus, inhibits Na^+-dependent Cl^- cotransporter-1 (NKCC1) and increases K^+:Cl^- cotransporter activity, leading to decreased $[Cl^-]_i$[44]. Thus, 3 different maneuvers that reduce $[Cl^-]_i$ increased pWNK4-RRxS levels, suggesting that WNK4-RRxS phosphorylation increases in response to $[Cl^-]_i$ depletion. It is thus likely that the known LKM-induced $[Cl^-]_i$ depletion[7] was responsible for increased WNK4-RRxS phosphorylation under this condition.

Changes in extracellular $[K^+]$ directly modulate levels of WNK4 S64 and S1196 in kidney

The kidney slice *ex vivo* system[45,46] was used to assess direct modulation by $[K^+]_e$. Higher pWNK4-S64 (Figure 6A–B) and pWNK4-S1196 levels (Figure 6C–D) were observed in freshly prepared kidney slices incubated in a low $[K^+]$ solution than in those on a normal $[K^+]$ solution. Higher pNCC levels were also observed as previously reported[45].

Kir5.1$^{-/-}$ mice present higher levels of NCC phosphorylation and activity[47,48]. Their DCT cells have higher basolateral K^+ conductance and a more negative membrane potential, which are expected to reduce $[Cl^-]_i$. These parameters, as well as the high pNCC levels are not normalized by high K^+ diet, which does normalize plasma $[K^+]$[47]. Thus, we investigated pWNK4-RRxS levels in these mice. As shown in Figure 6E–F, kidney levels of WNK4 were slightly higher, although not significantly different in Kir5.1$^{-/-}$ mice. However, both pWNK4-S64/WNK4 and pWNK4-S1196/WNK4 ratios were significantly higher. Thus, membrane potential variations in DCT cells that are expected to reduce $[Cl^-]_i$ can lead to increases in pWNK4 at S64 and S1196 levels.

Changes in $[Cl^-]_i$ can modulate KLHL3-CUL3 E3 activity and therefore WNK4 and KS-WNK1 levels

Mice maintained on a LKD have higher phosphorylation levels of KLHL3 at the S433 site of the substrate binding domain[31] that prevents interaction with WNK4 and decreases KLHL3-targeted degradation[34]. Accordingly, mice on an LKD display higher kidney WNK4[31] and KS-WNK1[49] protein levels than mice on normal K^+ diet. We investigated whether KLHL3 phosphorylation at the S433 site and KLHL3-targeted degradation of WNK4 is modulated by changes in $[Cl^-]_i$ in HEK293 cells. Incubation with LKM promoted an increase in WNK4 abundance only in the presence of KLHL3, which suggests KLHL3 activity (WNK4 degradation) is inhibited by low $[K^+]_e$ (Figure 7A–B). Similarly, WNK4 levels were increased by hypotonic low Cl^- medium incubation, a phenomenon that was significantly magnified by KLHL3 transfection (Figure 7C–D). Thus, these results suggest that WNK4 abundance can be regulated by $[Cl^-]_i$ in a KLHL3 dependent manner. Accordingly, increased KLHL3-S433 inhibitory phosphorylation was observed in cells exposed to hypotonic low Cl^- medium (Figure 7E), suggesting that changes in $[Cl^-]_i$ may underlie the modulation of KLHL3 phosphorylation and activity observed in mice on LKD[31].

Thomson et al.[39] have recently shown that WNK4$^{-/-}$ mice have large WNK bodies in the DCT that are still present when plasma $[K^+]$ levels are corrected by a high K^+ diet. We reasoned that WNK4$^{-/-}$ mice may have higher levels of KS-WNK1 protein that drive

the formation of WNK bodies since the formation of these structures is dependent on the presence of this protein[38]. This was indeed the case (Figure 8A). Because KS-WNK1 is very sensitive to KLHL3-targeted degradation[49,50] and expression of KS-WNK1 and KLHL3 is restricted to the DCT[15,51,52], the level of KS-WNK1 expression may be a good indicator of KLHL3-CUL3 E3 activity. We thus hypothesized that low $[Cl^-]_i$ in the DCTs of WNK4$^{-/-}$ mice may be responsible for the high KS-WNK1 levels.

To investigate this hypothesis, we administered thiazides to mice, reasoning that this would lower $[Cl^-]_i$ of DCT cells as NCC is the mayor pathway for Cl^- entry. Supporting this, a mathematical model of the DCT predicts that blockade of 99 % of NCC function would lead to a reduction in $[Cl^-]_i$ from 18.5 mM at baseline conditions to 12.1 mM (A. Weinstein personal communication: unpublished from the calculations in Weinstein, 2018[53]). After a 12-hour treatment period, plasma $[K^+]$ was similar among thiazide-treated and vehicle-treated mice, but higher pNCC levels (perhaps due to $[Cl^-]_i$ depletion) were observed in the hydrochlorothiazide group. Moreover, slightly increased KS-WNK1 levels were observed (Figure 8B) and WNK bodies were detected (Figure 8C–D). Thus, acute thiazide treatment in mice, which is predicted to decrease DCT $[Cl^-]_i$, leads to increased pNCC, increased KS-WNK1 protein levels, and formation of WNK bodies that may be indicative of decreased KLHL3-targeted degradation.

DISCUSSION

WNK4's inhibition by direct Cl^- binding is the currently accepted mechanism by which NCC phosphorylation is regulated in response to changes in $[K^+]_e$. The first direct *in vivo* evidence supporting this mechanism came with the generation of WNK4$^{L319F/L321F}$ mice, which present a familial hyperkalemic hypertension-like phenotype, with the inability to upregulate NCC by low K^+ intake[54]. In the present work we generated a mouse model harboring a different Cl^--insensitive WNK4 mutant and, as performed by Chen et al.[54], we evaluated the ability of these mice to activate the SPAK/OSR1-NCC pathway in response to LKD. In contrast to what Chen et al. reported, our mice did not display elevated plasma $[K^+]$ or $[Cl^-]$ (Table 1) at baseline, and only presented slightly higher pNCC levels (Figure 1). This might be due to differences in diet composition or genetic background, as suggested by our observation that the WNK4-L319F mutation in a mixed B6–129/Sv background did result in mild hyperkalemia. However, we cannot rule out that the phenotypic differences may be due to the additional mutation introduced in the mice generated by Chen et al. (L321F). In *in vitro* experiments it has been observed that the equivalent mutation to L321F in WNK1 and hWNK4 does not alter kinase activity[28,30] and in *Xenopus laevis* oocytes the single mutant L319F has the same effect as the double mutant L319F/L321F on its ability to activate NCC[28]. Nevertheless, side by side comparison (in the same lab) of the effects of these mutations in mice on the same background and will be necessary to rule out this possibility.

Another substantial difference from the results reported by Chen et al. is that we observed that WNK4-L319F mice could clearly upregulate pNCC when given LKD (Figure 2). This could be related to the magnitude of the fall in plasma $[K^+]$, which can in turn be due to the duration of the dietary regime (4 days vs. 7 days). In the report by Chen et al.,

WNK4-L319F,L321F mice still displayed higher plasma $[K^+]$ when compared to WT mice when kept on LKD. Anyhow, our experiments do not discard that direct binding of Cl^- to WNK4 is one of the key mechanisms involved in NCC regulation by $[K^+]_e$, but support the idea that additional mechanisms participate. The relevance of each of these mechanisms may depend on the temporal length of the physiological challenge.

In the present work we begin to explore these other mechanisms. First, we show that WNK4 phosphorylation at the S64 and S1196 sites increases in mice maintained on a LKD, and this increase occurs in response to direct sensing of $[K^+]_e$ by DCT cells since it was also observed in kidney slices and WNK4-transfected HEK293 cells incubated in a LKM. Additionally, in HEK293 cells, three different maneuvers that produce $[Cl^-]_i$ depletion stimulated WNK4-RRxS phosphorylation. Thus, the $[Cl^-]_i$ depletion that occurs in response to incubation in LKM in these cells[7] probably mediated the increases observed in WNK4 S64 and S1196 phosphorylation under this condition as well. Supporting that DCT $[Cl^-]_i$ depletion may be behind the increased WNK4-RRxS phosphorylation observed in mice on LKD, increased levels of pWNK4 at S64 and S1196 were observed in Kir5.1$^{-/-}$ mice that have been shown to have higher DCT basolateral K^+ conductance and hyperpolarized membranes that are expected to result in reductions in $[Cl^-]_i$ [47]. Thus, modulation of WNK4 activity through RRxS phosphorylation may contribute to NCC upregulation under LKD.

Another pathway that may also be relevant in LKD-induced NCC activation involves regulation of WNK kinases levels in DCT, through the modulation of KLHL3-CUL3 E3 activity. Kidney WNK4 and KS-WNK1 protein levels have been shown to increase in mice on LKD[31,49], and according to Ishizawa et al. phosphorylation of the substrate binding domain of KLHL3, that prevents WNK binding, increases in mice on LKD[31]. Here we show that this modulation of KLHL3-targeted degradation may occur in response to low $[K^+]_e$-induced decreases in $[Cl^-]_i$, given that in our experiments performed in HEK293 cells, $[Cl^-]_i$ depletion promoted KLHL3-S433 phosphorylation and inhibited KLHL3-targeted degradation of WNK4 (Figure 7). Although definitive evidence of the *in vivo* role of modulation of KLHL3-CUL3 E3 activity by $[Cl^-]_i$ is necessary, we propose that the observed high levels of KS-WNK1 in WNK4$^{-/-}$ mice, and the KS-WNK1 upregulation observed in mice acutely treated with thiazides, may be explained by this mechanism, given that, as discussed above, KS-WNK1 protein levels in the kidney are a good indicator of the activity level of the KLHL3-CUL3 E3 complex[15,51,52,49,50].

Finally, the high KS-WNK1 levels observed in WNK4$^{-/-}$ mice that also present large WNK bodies in their DCTs adds up to the existing evidence suggesting that the induction of KS-WNK1 expression promotes the formation of these structures. This evidence includes the observation that in other models, like mice on LKD and KLHL3-R528H knockin mice, high KS-WNK1 protein levels correlate with the observation of WNK bodies[38,39,49]. Moreover, absence of WNK bodies in KS-WNK1 knockout mice on LKD suggest that this protein plays a key scaffolding role within these structures[38]. Thus, observation of WNK bodies may serve as a surrogate for detection of KS-WNK1 induction.

In summary, this work shows that release of Cl^- ions from WNK4's active site is probably not the only mechanism involved in the activation of NCC under low $[K^+]_e$. We propose

that additional mechanisms may involve WNK4 and KLHL3 phosphorylation at RRXS sites that modulate kinase's activity and expression levels, respectively. Our data suggests that these additional pathways may be modulated by $[Cl^-]_i$, which plays a central role in the ion-sensitive signaling of DCT cells (Figure 9). These mechanisms could be working in parallel in order to ensure NCC activation during low K^+ intake and prevent urinary K^+ loss. Accordingly, in vitro experiments show that WNK4 L319F needs to be phosphorylated in RRxS motifs in order to display high kinase activity [35]. Alternatively, they might activate at different time points. For example, Cl^- dissociation from WNK4 could mediate rapid responses, as changes in $[Cl^-]_i$ seem to be transient [55] and perhaps WNK4 and KLHL3 phosphorylation could be important for longer periods of time. Finally, it is noteworthy that this implies that yet undescribed Cl^- sensitive molecules may exist in the DCT that participate in these signaling pathways. Further experiments will be necessary to identify these molecules and to address if one of the proposed mechanisms predominates over the other.

Supplementary Material

Refer to Web version on PubMed Central for supplementary material.

ACKNOWLEDGEMETS

Adrián Rafael Murillo-de-Ozores is a doctoral student from the "Programa de Doctorado en Ciencias Biomédicas, Universidad Nacional Autónoma de México (UNAM)" and received a fellowship 606808 from CONACYT. We thank Dr. Dario Alessi for kindly gifting us the WNK463 inhibitor. We thank Cristino Cruz for his help with the measurement of electrolytes in mouse plasma samples and Maria Cristina Díaz Vergara for her technical support. We thank Mariela Guadalupe Contreras Escamilla, Berenice Díaz Ramos, Marysol González Yáñez, Tania Pérez Benhumea, and Anahi Leticia Aguilar Lopez from the animal facility for their help with the wild type and transgenic mice colonies. We thank the "Red de Apoyo a la Investigación" for providing access to the cell culture facility. This work was supported by the grants from Conacyt Mexico No. 101720 to MCB and A1-S-8290 to GG, the grant from PAPIIT UNAM No. IN201519 to GG, the grants form NIH No. DK51496 to GG and DHE, DK054983-15 and U54TR001628 to DHE, DK115366 to DHL, and DK093501 to ED, the grant I01BX002228 from the Department of Veterans Affairs, and the grant from Leducq Foundation No. 17CVD05 to ED and DHE.

ARMO, MCB, and GG conceived and designed the study. ARMO, HCC, GRMA, RV, LIGM, NV, ALS, DHL, WHW, ED, DHE, GG, MCB collected, analyzed, and interpreted the data. ARMO, GG, and MCB wrote the manuscript. All authors approved the final version of the manuscript.

Part of this work was previously presented in a poster presentation at the 2021 Kidney Week organized by the American Society of Nephrology (PO1083).

REFERENCES

1. Mente A, O'Donnell MJ, Rangarajan S, et al. Association of Urinary Sodium and Potassium Excretion with Blood Pressure. N Engl J Med. 2014;371(7):601–611. doi:10.1056/NEJMoa1311989 [PubMed: 25119606]
2. Sacks FM, Svetkey LP, Vollmer WM, et al. Effects on blood presure of reduced dietary sodium and the dietary approaches to stop hypertension (DASH) diet. New Engl J Med. 2001;344(1):3–10. [PubMed: 11136953]
3. Neal B, Wu Y, Feng X, et al. Effect of Salt Substitution on Cardiovascular Events and Death. N Engl J Med. 2021;385(12):1067–1077. doi:10.1056/nejmoa2105675 [PubMed: 34459569]
4. O'Donnell M, Mente A, Rangarajan S, et al. Urinary Sodium and Potassium Excretion, Mortality, and Cardiovascular Events. N Engl J Med. 2014;371(7):612–623. doi:10.1056/NEJMoa1311889 [PubMed: 25119607]

5. Guyton AC. Blood pressure control - Special role of the kidneys and body fluids. Science (80-). 1991;252(5014):1813–1816. doi:10.1126/science.2063193
6. Vitzthum H, Seniuk A, Schulte LH, Müller ML, Hetz H, Ehmke H. Functional coupling of renal K+ and Na+ handling causes high blood pressure in Na+ replete mice. J Physiol. 2014;592:1139–1157. doi:10.1113/jphysiol.2013.266924 [PubMed: 24396058]
7. Terker AS, Zhang C, McCormick JA, et al. Potassium modulates electrolyte balance and blood pressure through effects on distal cell voltage and chloride. Cell Metab. 2015;21(1):39–50. doi:10.1016/j.cmet.2014.12.006 [PubMed: 25565204]
8. Gamba G.Molecular Physiology and Pathophysiology of Electroneutral Cation-Chloride Cotransporters. Physiol Rev. 2005;85(2):423–493. doi:10.1152/physrev.00011.2004 [PubMed: 15788703]
9. Murillo-de-Ozores AR, Gamba G, Castañeda-Bueno M. Molecular mechanisms for the regulation of blood pressure by potassium. In: Current Topics in Membranes. Vol 83. 1st ed. Elsevier Inc.; 2019:285–313. doi:10.1016/bs.ctm.2019.01.004 [PubMed: 31196607]
10. Simon DB, Nelson-Williams C, Bia MJ, et al. Gitelman's variant of Bartter's syndrome, inherited hypokalaemic alkalosis, is caused by mutations in the thiazide-sensitive Na-Cl cotransporter. Nat Genet. 1996;12(1):24–30. doi:10.1038/ng0196-24 [PubMed: 8528245]
11. Lalioti MD, Zhang J, Volkman HM, et al. Wnk4 controls blood pressure and potassium homeostasis via regulation of mass and activity of the distal convoluted tubule. Nat Genet. 2006;38(10):1124–1132. doi:10.1038/ng1877 [PubMed: 16964266]
12. Grimm PR, Coleman R, Delpire E, Welling PA. Constitutively Active SPAK Causes Hyperkalemia by Activating NCC and Remodeling Distal Tubules. J Am Soc Nephrol. 2017;28(9):2597–2606. doi:10.1681/ASN.2016090948 [PubMed: 28442491]
13. Wilson FH, Disse-Nicodèm S, Choate KA, et al. Human Hypertension Caused by Mutations in WNK Kinases. Science (80-). 2001;293(5532):1107–1112. doi:10.1126/science.1062844
14. Boyden LM, Choi M, Choate KA, et al. Mutations in kelch-like 3 and cullin 3 cause hypertension and electrolyte abnormalities. Nature. 2012;482(7383):98–102. doi:10.1038/nature10814 [PubMed: 22266938]
15. Louis-Dit-Picard H, Barc J, Trujillano D, et al. KLHL3 mutations cause familial hyperkalemic hypertension by impairing ion transport in the distal nephron. Nat Genet. 2012;44(4):456–460. doi:10.1038/ng.2218 [PubMed: 22406640]
16. Pacheco-Alvarez D, San Cristóbal P, Meade P, et al. The Na+:Cl- cotransporter is activated and phosphorylated at the amino-terminal domain upon intracellular chloride depletion. J Biol Chem. 2006;281(39):28755–28763. doi:10.1074/jbc.M603773200
17. Alessi DR, Zhang J, Khanna A, Hochdorfer T, Shang Y, Kahle KT. The WNK-SPAK/OSR1 pathway: Master regulator of cation-chloride cotransporters. Sci Signal. 2014;7(334):re3-re3. doi:10.1126/scisignal.2005365
18. Vitari AC, Deak M, Morrice NA, Alessi DR. The WNK1 and WNK4 protein kinases that are mutated in Gordon's hypertension syndrome phosphorylate and activate SPAK and OSR1 protein kinases. Biochem J. 2005;391(1):17–24. doi:10.1042/BJ20051180 [PubMed: 16083423]
19. Castaneda-Bueno M, Cervantes-Perez LG, Vazquez N, et al. Activation of the renal Na+:Cl- cotransporter by angiotensin II is a WNK4-dependent process. Proc Natl Acad Sci. 2012;109(20):7929–7934. doi:10.1073/pnas.1200947109 [PubMed: 22550170]
20. Susa K, Sohara E, Takahashi D, Okado T, Rai T, Uchida S. WNK4 is indispensable for the pathogenesis of pseudohypoaldosteronism type II caused by mutant KLHL3. Biochem Biophys Res Commun. 2017;491(3):727–732. doi:10.1016/j.bbrc.2017.07.121 [PubMed: 28743496]
21. Murillo-de-Ozores AR, Rodríguez-Gama A, Carbajal-Contreras H, Gamba G, Castañeda-Bueno M. WNK4 kinase: from structure to physiology. Am J Physiol Physiol. 2021;320(3):F378–F403. doi:10.1152/ajprenal.00634.2020
22. Vallon V, Schroth J, Lang F, Kuhl D, Uchida S. Expression and phosphorylation of the Na+-Cl- cotransporter NCC in vivo is regulated by dietary salt, potassium, and SGK1. Am J Physiol - Ren Physiol. 2009;297(3):F704–F712. doi:10.1152/ajprenal.00030.2009

23. Sorensen MV, Grossmann S, Roesinger M, et al. Rapid dephosphorylation of the renal sodium chloride cotransporter in response to oral potassium intake in mice. Kidney Int. 2013;83(5):811–824. doi:10.1038/ki.2013.14 [PubMed: 23447069]
24. Castaneda-Bueno M, Cervantes-Perez LG, Rojas-Vega L, et al. Modulation of NCC activity by low and high K+ intake: insights into the signaling pathways involved. Am J Physiol - Ren Physiol. 2014;306(12):F1507-F1519. doi:10.1152/ajprenal.00255.2013
25. Cuevas CA, Su X-T, Wang M-X, et al. Potassium Sensing by Renal Distal Tubules Requires Kir4.1. J Am Soc Nephrol. 2017;28(6):1814–1825. doi:10.1681/ASN.2016090935 [PubMed: 28052988]
26. Wang MX, Cuevas CA, Su XT, et al. Potassium intake modulates the thiazide-sensitive sodium-chloride cotransporter (NCC) activity via the Kir4.1 potassium channel. Kidney Int. 2018;93(4):893–902. doi:10.1016/j.kint.2017.10.023 [PubMed: 29310825]
27. Nomura N, Shoda W, Wang Y, et al. Role of ClC-K and barttin in low-potassium induced sodium-chloride cotransporter activation and hypertension in mouse kidney. Biosci Rep. 2018;38(1). doi:10.1042/BSR20171243
28. Bazua-Valenti S, Chavez-Canales M, Rojas-Vega L, et al. The Effect of WNK4 on the Na+-Cl- Cotransporter Is Modulated by Intracellular Chloride. J Am Soc Nephrol. 2015;26(8):1781–1786. doi:10.1681/ASN.2014050470 [PubMed: 25542968]
29. Terker AS, Zhang C, Erspamer KJ, Gamba G, Yang C-L, Ellison DH. Unique chloride-sensing properties of WNK4 permit the distal nephron to modulate potassium homeostasis. Kidney Int. 2015;89(1):1–8. doi:10.1038/ki.2015.289
30. Piala AT, Moon TM, Akella R, He H, Cobb MH, Goldsmith EJ. Chloride Sensing by WNK1 Involves Inhibition of Autophosphorylation. Sci Signal. 2014;7(324):ra41–ra41. doi:10.1126/scisignal.2005050 [PubMed: 24803536]
31. Ishizawa K, Xu N, Loffing J, et al. Potassium depletion stimulates Na-Cl cotransporter via phosphorylation and inactivation of the ubiquitin ligase Kelch-like 3. Biochem Biophys Res Commun. 2016;480(4):745–751. doi:10.1016/j.bbrc.2016.10.127 [PubMed: 27942049]
32. Shibata S, Zhang J, Puthumana J, Stone KL, Lifton RP. Kelch-like 3 and Cullin 3 regulate electrolyte homeostasis via ubiquitination and degradation of WNK4. Proc Natl Acad Sci. 2013;110(19):7838–7843. doi:10.1073/pnas.1304592110 [PubMed: 23576762]
33. Wakabayashi M, Mori T, Isobe K, et al. Impaired KLHL3-mediated ubiquitination of WNK4 causes human hypertension. Cell Rep. 2013;3(3):858–868. doi:10.1016/j.celrep.2013.02.024 [PubMed: 23453970]
34. Shibata S, Arroyo JP, Castaneda-Bueno M, et al. Angiotensin II signaling via protein kinase C phosphorylates Kelch-like 3, preventing WNK4 degradation. Proc Natl Acad Sci. 2014;111(43):15556–15561. doi:10.1073/pnas.1418342111
35. Castañeda-Bueno M, Arroyo JP, Zhang J, et al. Phosphorylation by PKC and PKA regulate the kinase activity and downstream signaling of WNK4. Proc Natl Acad Sci. 2017;114(5):E879–E886. doi:10.1073/pnas.1620315114 [PubMed: 28096417]
36. Bazúa-Valenti S, Gamba G. Revisiting the NaCl cotransporter regulation by with-no-lysine kinases. Am J Physiol - Cell Physiol. 2015;308(10):C779–C791. doi:10.1152/ajpcell.00065.2015 [PubMed: 25788573]
37. Yang YS, Xie J, Yang Sen S, Lin SH, Huang CL. Differential roles of WNK4 in regulation of NCC in vivo. Am J Physiol - Ren Physiol. 2018;314(5):F999-F1007. doi:10.1152/ajprenal.00177.2017
38. Boyd-Shiwarski CR, Shiwarski DJ, Roy A, et al. Potassium-regulated distal tubule WNK bodies are kidney-specific WNK1 dependent. Mol Biol Cell. 2018;29(4):499–509. doi:10.1091/mbc.E17-08-0529 [PubMed: 29237822]
39. Thomson MN, Cuevas CA, Bewarder TM, et al. WNK bodies cluster WNK4 and SPAK/OSR1 to promote NCC activation in hypokalemia. Am J Physiol Physiol. 2020;318(1):F216–F228. doi:10.1152/ajprenal.00232.2019
40. Richardson C, Rafiqi FH, Karlsson HKR, et al. Activation of the thiazide-sensitive Na+-Cl- cotransporter by the WNK-regulated kinases SPAK and OSR1. J Cell Sci. 2008;121(5):675–684. doi:10.1242/jcs.025312 [PubMed: 18270262]

41. Gagnon KBE, England R, Delpire E. Characterization of SPAK and OSR1, Regulatory Kinases of the Na-K-2Cl Cotransporter. Mol Cell Biol. 2006;26(2):689–698. doi:10.1128/MCB.26.2.689-698.2006 [PubMed: 16382158]
42. Conway LC, Cardarelli RA, Moore YE, et al. N-Ethylmaleimide increases KCC2 cotransporter activity by modulating transporter phosphorylation. J Biol Chem. 2017;292(52):21253–21263. doi:10.1074/jbc.M117.817841
43. Yamada K, Park H-M, Rigel DF, et al. Small-molecule WNK inhibition regulates cardiovascular and renal function. Nat Chem Biol. 2016;12(11):896–898. doi:10.1038/nchembio.2168 [PubMed: 27595330]
44. Mayes-Hopfinger L, Enache A, Xie J, et al. Chloride sensing by WNK1 regulates NLRP3 inflammasome activation and pyroptosis. Nat Commun. 2021;12(1):1–17. doi:10.1038/s41467-021-24784-4 [PubMed: 33397941]
45. Penton D, Czogalla J, Wengi A, et al. Extracellular K + rapidly controls NaCl cotransporter phosphorylation in the native distal convoluted tubule by Cl − -dependent and independent mechanisms. J Physiol. 2016;594(21):6319–6331. doi:10.1113/JP272504 [PubMed: 27457700]
46. Mukherjee A, Yang C-L, McCormick JA, Martz K, Sharma A, Ellison DH. Roles of WNK4 and SPAK in K + mediated dephosphorylation of the sodium chloride cotransporter. Am J Physiol Physiol. 2021. doi:10.1152/ajprenal.00459.2020
47. Wu P, Gao ZX, Zhang DD, Su XT, Wang WH, Lin DH. Deletion of Kir5.1 impairs renal ability to excrete potassium during increased dietary potassium intake. J Am Soc Nephrol. 2019;30(8):1425–1438. doi:10.1681/ASN.2019010025 [PubMed: 31239388]
48. Paulais M, Bloch-Faure M, Picard N, et al. Renal phenotype in mice lacking the Kir5.1 (Kcnj16) K+ channel subunit contrasts with that observed in SeSAME/EAST syndrome. Proc Natl Acad Sci. 2011;108(25):10361–10366. doi:10.1073/pnas.1101400108
49. Ostrosky-Frid M, Chávez-Canales M, Zhang J, et al. Role of KLHL3 and dietary K + in regulating KS-WNK1 expression. Am J Physiol Physiol. 2021;320(5):F734–F747. doi:10.1152/ajprenal.00575.2020
50. Louis-Dit-Picard H, Kouranti I, Rafael C, et al. Mutation affecting the conserved acidic WNK1 motif causes inherited hyperkalemic hyperchloremic acidosis. J Clin Invest. 2020;130(12):6379–6394. doi:10.1172/JCI94171 [PubMed: 32790646]
51. Vidal-Petiot E, Cheval L, Faugeroux J, et al. A new methodology for quantification of alternatively spliced exons reveals a highly tissue-specific expression pattern of WNK1 isoforms. PLoS One. 2012;7(5):1–9. doi:10.1371/journal.pone.0037751
52. Chen L, Chou C, Knepper MA. A Comprehensive Map of mRNAs and Their Isoforms across All 14 Renal Tubule Segments of Mouse. J Am Soc Nephrol. 2021;32(4):897–912. doi:10.1681/ASN.2020101406 [PubMed: 33769951]
53. Weinstein AM. A mathematical model of distal nephron acidification: Diuretic effects. Am J Physiol - Ren Physiol. 2008;295(5):1353–1364. doi:10.1152/ajprenal.90356.2008
54. Chen J-C, Lo Y-F, Lin Y-W, Lin S-H, Huang C-L, Cheng C-J. WNK4 kinase is a physiological intracellular chloride sensor. Proc Natl Acad Sci. 2019;116(10):4502–4507. doi:10.1073/pnas.1817220116 [PubMed: 30765526]
55. Su X, Klett NJ, Sharma A, et al. Distal convoluted tubule Cl − concentration is modulated via K + channels and transporters. Am J Physiol Physiol. 2020;319(3):F534–F540. doi:10.1152/ajprenal.00284.2020

TRANSLATIONAL STATEMENT

Modulation of the NaCl cotransporter (NCC) activity by dietary K^+ explain, at least in part, the inverse relationship between K^+ ingestion and blood pressure levels. Here we describe novel molecular mechanisms that are involved in this regulation that include modulation of With-No-Lysine 4 (WNK4) activity by phosphorylation of sites within its regulatory domains, and modulation of WNK4/KS-WNK1 degradation by the KLHL3-CUL3 E3 ubiquitin ligase, through phosphorylation of KLHL3's substrate binding domain. Our data suggest that $[K^+]_e$-induced changes in $[Cl^-]_i$ mediate activation of these alternative pathways, hinting that yet-unidentified Cl^- sensitive molecules may exist that are relevant for distal convoluted tubule physiology.

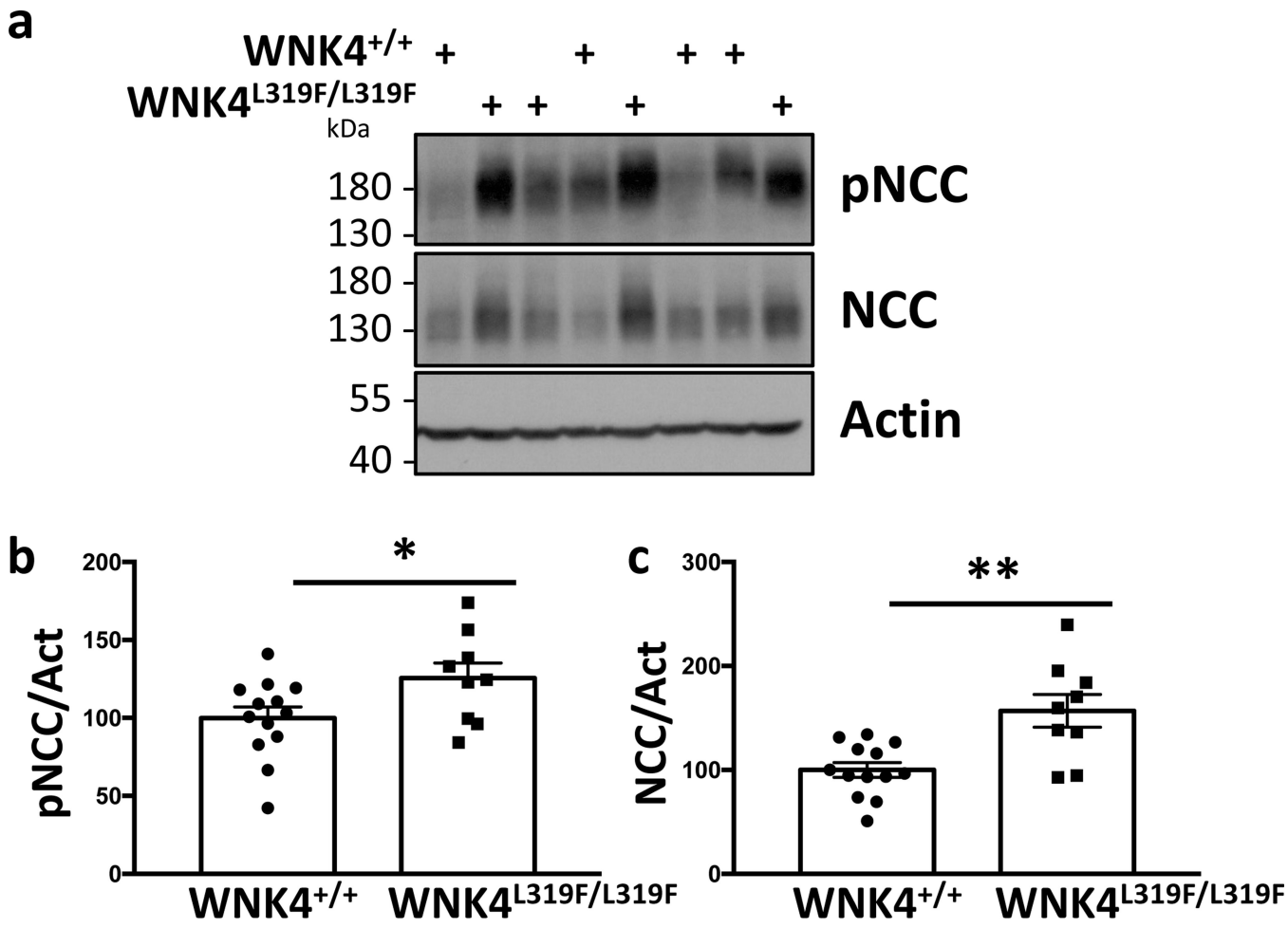

Figure 1.

Analysis of NCC and pNCC abundance in the kidneys from WT and WNK4$^{L319F/L319F}$ mice at baseline conditions. Representative immunoblots of NCC, pNCC (A) performed with total kidney lysates of wild type and WNK4$^{L319F/L319F}$ mice. Quantitative analysis of pNCC/Actin (B) and NCC/Actin (C) levels observed in immunoblots represented in (A). Values observed in wild type mice were normalized to 100%. Data are mean ± SEM. Two-tailed unpaired Student's t-test: *p<0.05, **p<0.005.

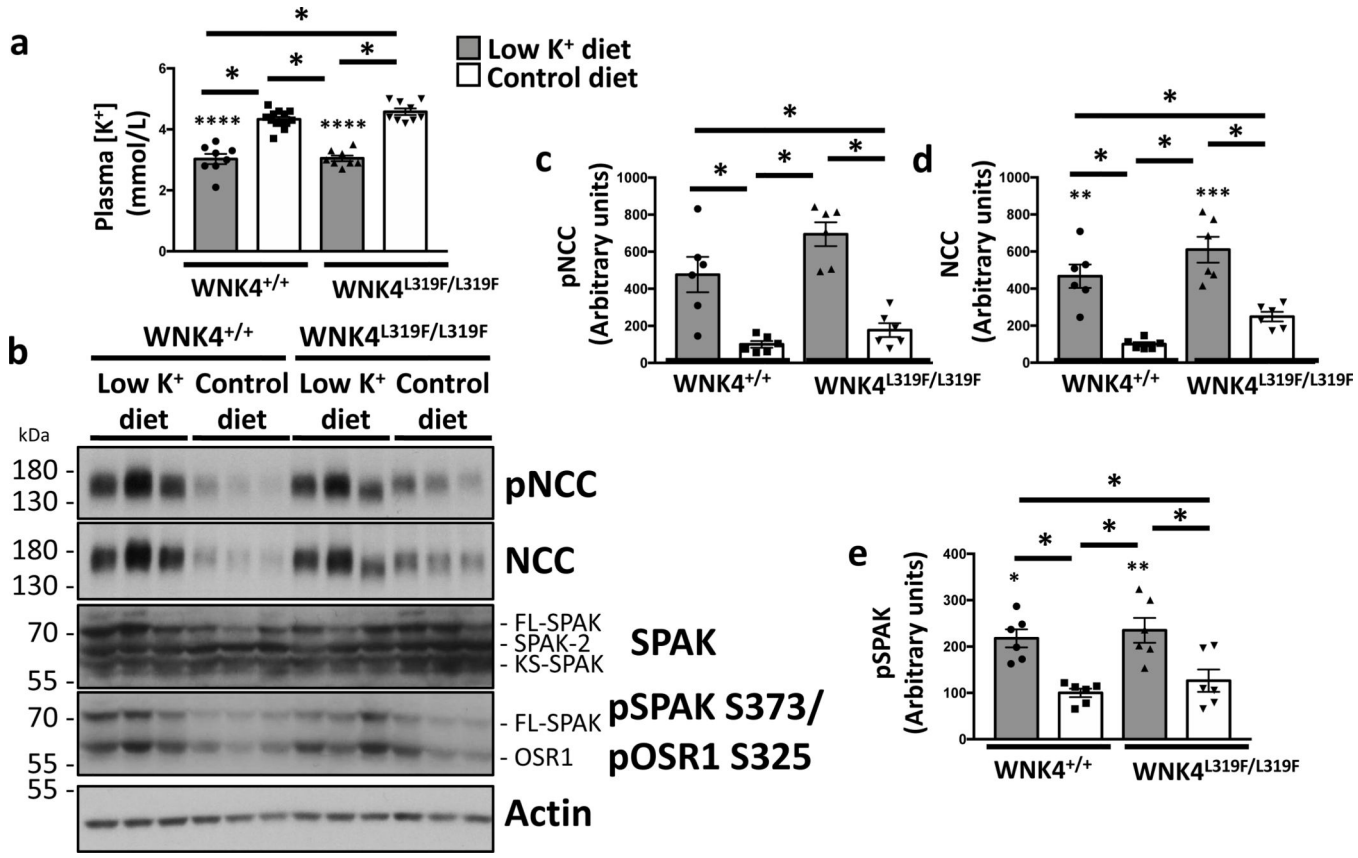

Figure 2.

Low $[K^+]_e$-induced upregulation of NCC expression and phosphorylation is observed in WNK4$^{L319F/L319F}$ mice. (A) WNK4$^{L319F/L319F}$ mice were placed on a normal or K^+ deficient diet for 7 days. No significant differences were observed in plasma $[K^+]$ among wild type and knockin mice maintained on normal K^+ diet. In both genotypes, administration of a K^+ deficient diet produced similar reductions in plasma $[K^+]$. (B) Representative immunoblots performed with total kidney lysates of wild type and WNK4$^{L319F/L319F}$ mice on normal and K^+ deficient diets. Quantitative analysis of pNCC/actin (C), NCC/actin levels (D) and pSPAK/actin (E) observed in immunoblots represented in B. Values observed in wild type mice on normal K^+ diet were normalized to 100% and other groups were normalized accordingly. Data are mean ± SEM. ANOVA with post hoc Tukey's Multiple comparison test: *$p < 0.05$ (total n=6).

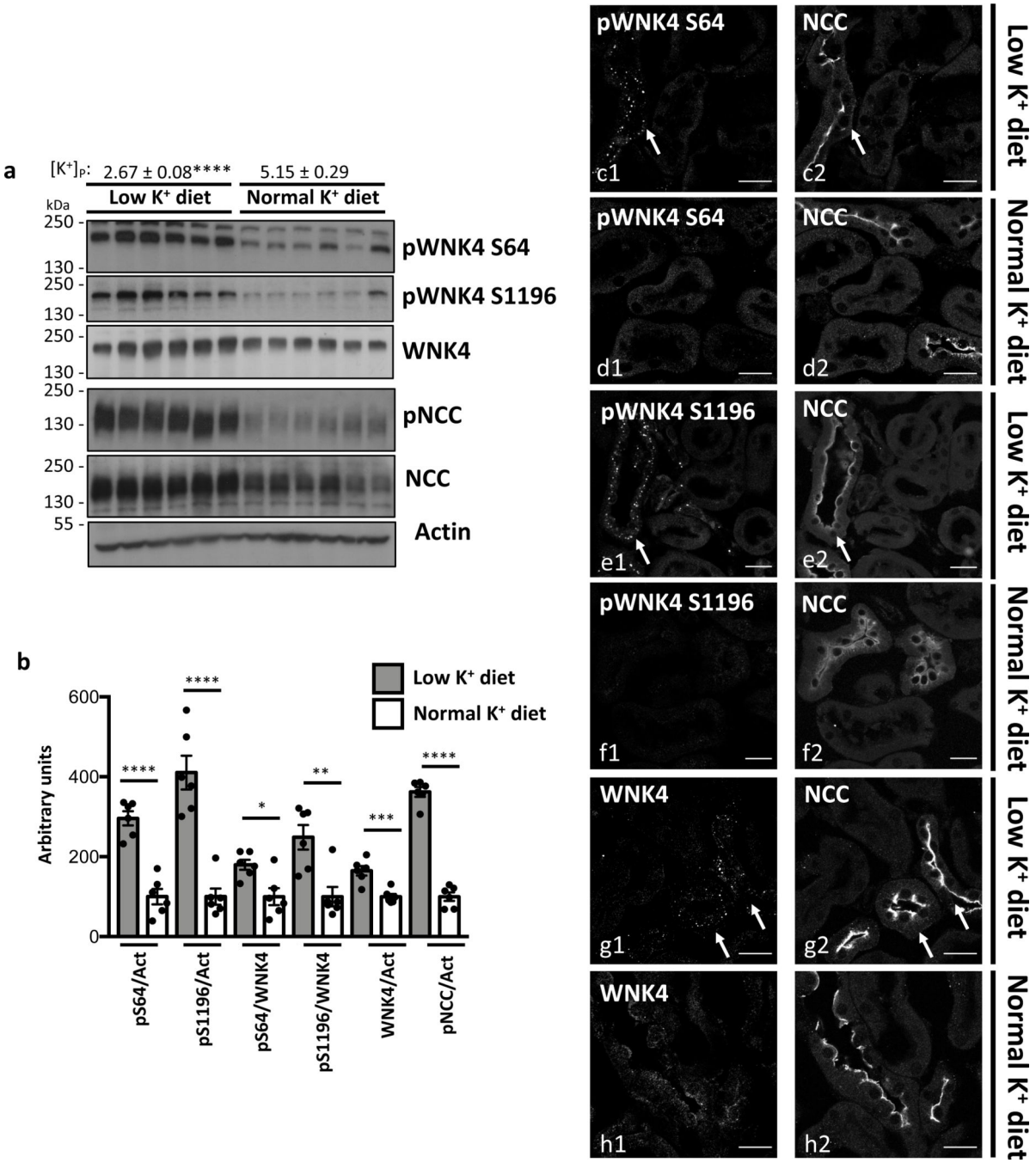

Figure 3.

WNK4 phosphorylation at S64 and S1196 is stimulated by low K^+ intake. (A) Representative immunoblots of total kidney proteins of mice maintained on normal K^+ diet (NKD) or low K^+ diet (LKD) for 7 days. Mean plasma [K^+] values for each group are shown on top of the blots. B) Results of the densitometric analysis of the blots represented in (A) show that WNK4 phosphorylation levels at S64 and S1196 are higher in mice on LKD even after normalization to total WNK4 levels. Ratio values obtained for mice on NKD were normalized to 100%. Bars represent mean and error bars represent SEM. For statistical

analysis, student t tests were performed. *p<0.01, **p<0.005, ***p<0.001, ****p<0.0001, n= 6 per group. (C-H) Immunofluorescent labeling of kidney slices from mice maintained on NKD or LKD was performed to detect changes that occur within DCT cells (identified by NCC labeling). WNK bodies were detected in DCT cells of mice maintained in LKD with the pWNK4-S64 (C), pS1196 (E), and WNK4 (G) antibodies, but were not detected in kidney slices from mice in NKD with these same antibodies (D, F, H).

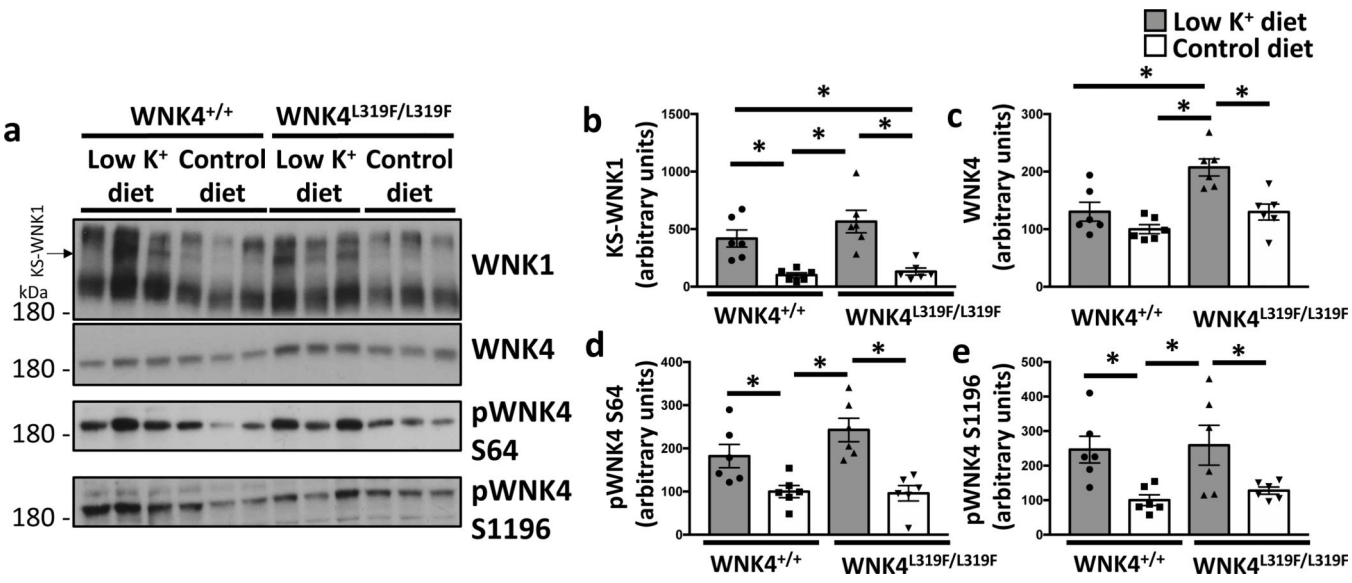

Figure 4.

Low [K^+] diet promotes the increase in WNK levels and WNK4 phosphorylation both in WT and $WNK4^{L319F/L319F}$ mice. (A) Representative immunoblots performed with total kidney lysates of wild type and $WNK4^{L319F/L319F}$ mice on normal and K^+ deficient diets. Quantitative analysis of WNK1/Coomassie (B), WNK4/actin (C), pWNK4-S64/actin (D) and pWNK4-S1196/actin (E) levels observed in immunoblots represented in A. The band corresponding to KS-WNK1 is indicated by an arrow and the identity of this band has been previously validated using KS-$WNK1^{-/-}$ mice[49]. Specificity of other bands observed in this blot has not been confirmed. Values observed in wild type mice on normal K^+ diet were normalized to 100% and other groups were normalized accordingly. Data are mean ± SEM. ANOVA with post hoc Tukey's Multiple comparison test: *$p < 0.05$ (total n=6).

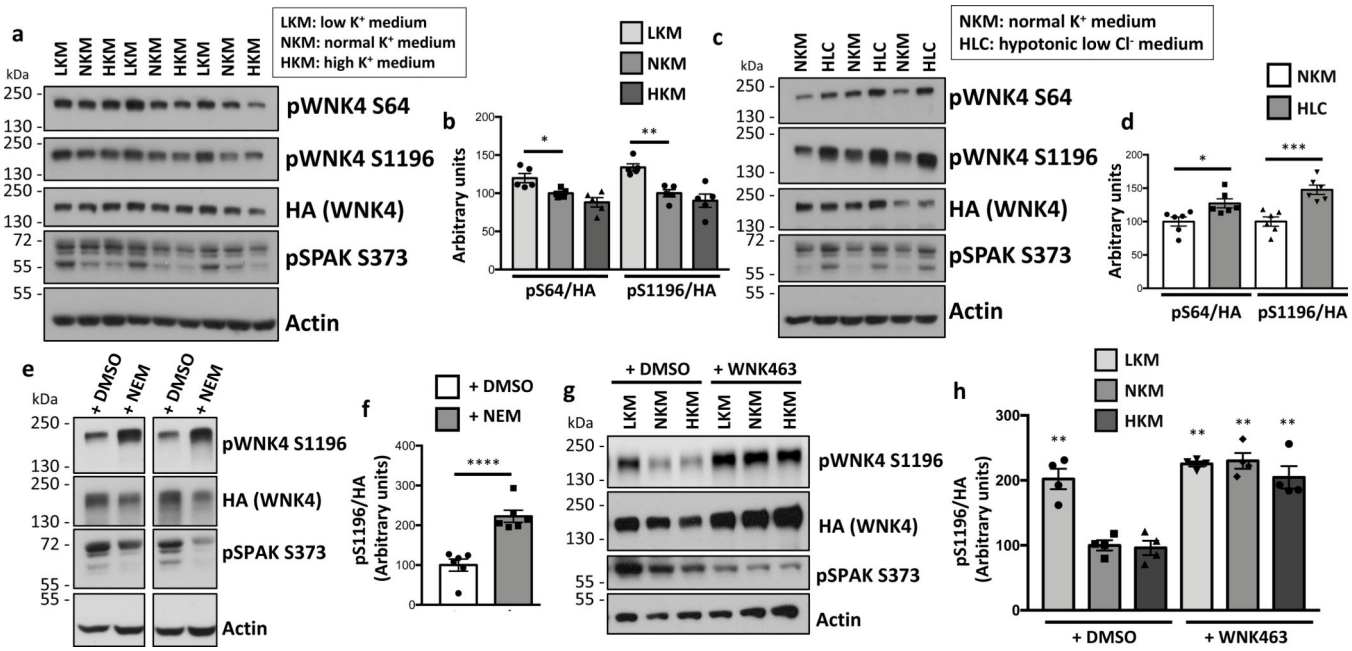

Figure 5.

Decreases in extracellular $[K^+]$ and intracellular $[Cl^-]_i$ stimulate WNK4-RRxS phosphorylation in HEK293 cells. (A) Representative immunoblots of WNK4-transfected HEK293 cells incubated on media containing 1mM K^+, 5mM K^+, or 10mM K^+ (LKM, NKM, or HKM, respectively). (B) Quantitation of pWNK4-S64/WNK4 and pWNK4-S1196/WNK4 from at least 5 independent experiments show a statistically significant increase in S64 and S1196 WNK4 phosphorylation in cells incubated in LKM. Values for NKM group were normalized to 100 % and other groups were normalized accordingly. Phosphorylation levels of SPAK/OSR1 were also altered as previously shown[7]. (C) Representative immunoblots of WNK4-transfected HEK293 cells incubated in NKM or hypotonic low Cl^- medium (HLC). (D) Densitometric analysis of the blots represented in C. At least 6 independent experiments were performed. Increased pWNK4-S64/WNK4 and pWNK4-S1196/WNK4 levels were observed in cells incubated in HLC medium. (E) Immunoblots of cells stimulated with N-ethylmaleimide (NEM, 100μM) for 30 minutes. (F) Results of quantitation, including data from at least 6 independent experiments. NEM stimulation decreases SPAK phosphorylation, as previously reported[42], but increases WNK4-S1196 phosphorylation. (G) Immunoblots of cells incubated in LKM, NKM, or HKM in the absence or presence of WNK463 (10μM). (H) Results of quantitation, including data from at least 4 experiments. All data are mean ± SEM. Two-tailed unpaired Student's t-test (two groups comparison) or ANOVA with post hoc Dunnett's Multiple comparison test (multiple groups comparison) : *p < 0.05, **p <0.005, *** p<0.001, ****p <0.0005.

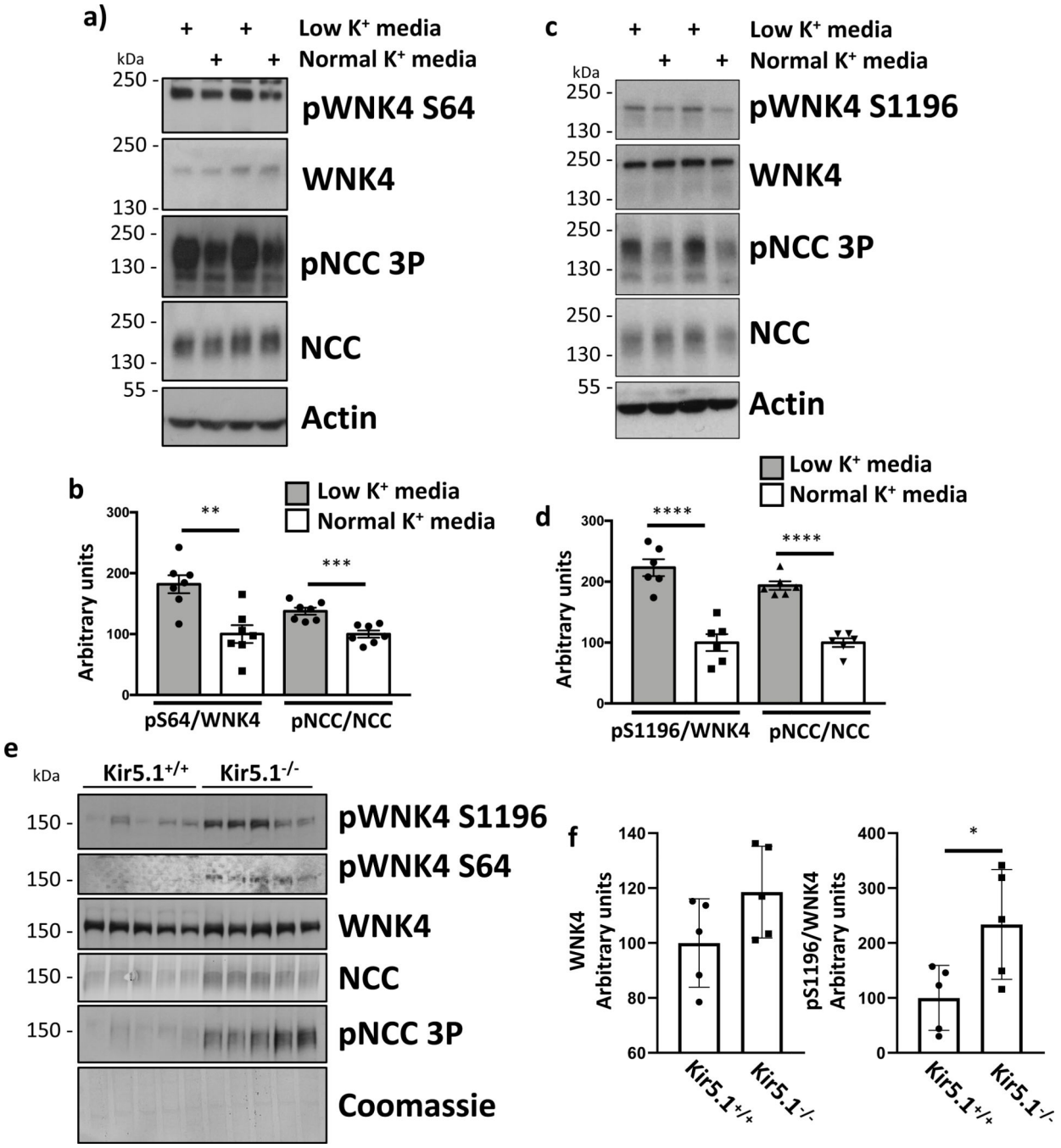

Figure 6.

WNK4 S64 and S1196 phosphorylation is directly modulated by $[K^+]_e$ in the kidney. (A) Representative immunoblots showing the levels of pWNK4-S64, WNK4, pNCC, and NCC of kidney slices incubated in normal K^+ (5 mM) and low K^+ (1 mM) containing buffers. (B) Results of quantitation of pWNK4-S64 and pNCC levels normalized to total protein levels. Ratio values for low K^+ samples were normalized to those observed on normal K^+ samples (100 %). (C) Same as in A, but pWNK4-S1196 levels were analyzed. (D) Results of quantitation of blots represented in (C). (F) Representative immunoblots of total

kidney protein samples from Kir5.1$^{+/+}$ and Kir5.1$^{-/-}$ mice. (G) Results of quantitation show statistically significant higher pWNK4-S1196/WNK4 levels in Kir5.1$^{-/-}$ mice. Data are mean ± SEM. Two-tailed unpaired Student's t-test: *p <0.05, **p <0.005, *** p <0.001, ****p < 0.0001.

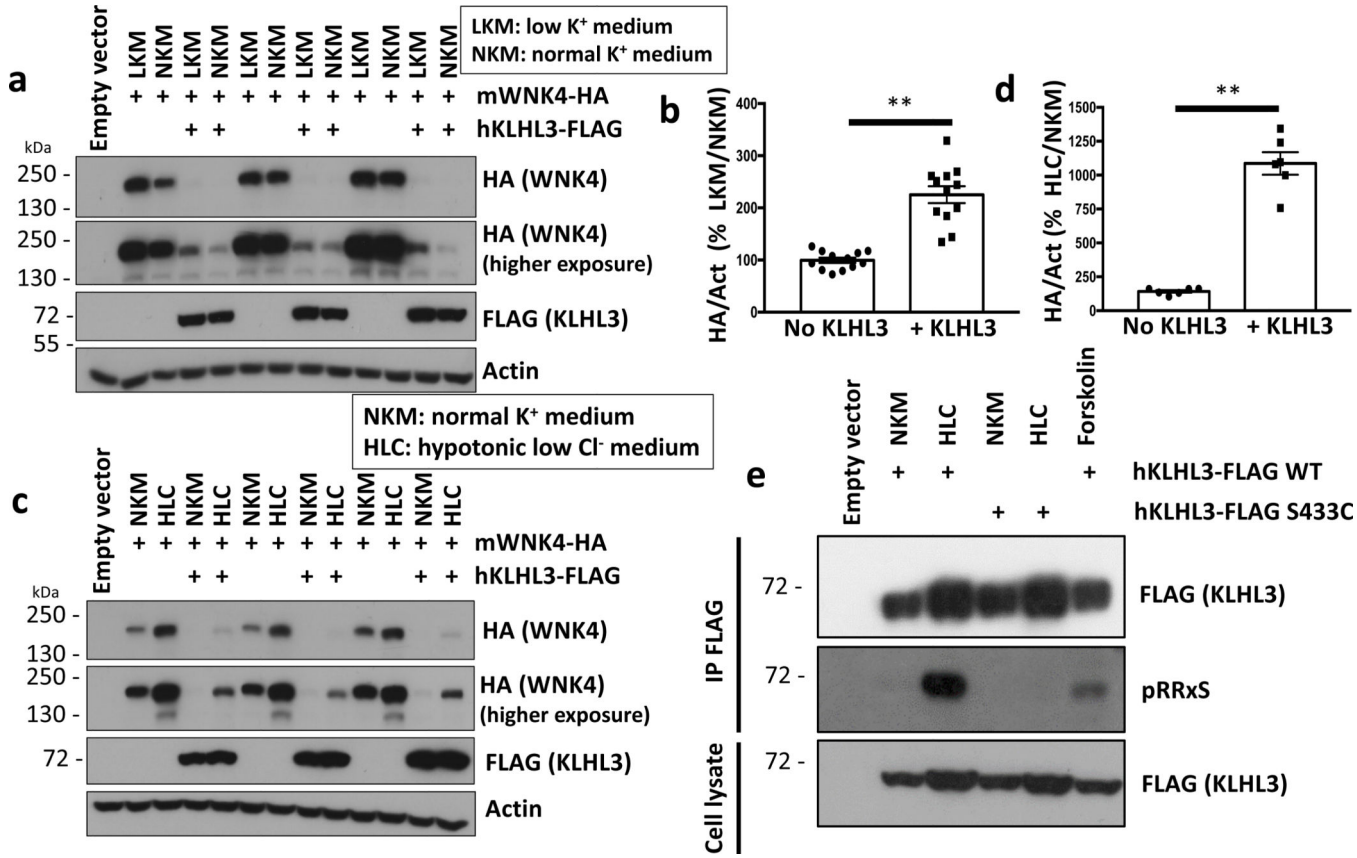

Figure 7.

KLHL3-targeted degradation of WNK kinases is modulated by $[Cl^-]_i$. (A) HEK293 cells were cotransfected with WNK4 plus empty vector or WNK4 plus KLHL3. After stimulation for 16 hours with the indicated media, cells were lysed and immunoblots were performed. (B) Results of quantitation of blots represented in (A) show that WNK4 levels are only modulated in response to changes in $[K^+]_e$ when KLHL3 is overexpressed. Bar graphs represent WNK4/Actin values observed in LKM, normalized to those observed in NKM. Two-tailed unpaired Student's t-test: **p <0.005 (C) Same as in A, but cells were stimulated with NKM or HLC medium. (D) Densitometric analysis shows that the upregulation of WNK4 protein levels observed in response to stimulation with HLC medium, is significantly higher in the presence of KLHL3. Two-tailed unpaired Student's t-test: **p <0.005 (E) Immunoprecipitation of FLAG-KLHL3 and blot with pRRxS antibody shows that KLHL3-S433 phosphorylation is increased by incubation with HLC medium. Transfection of KLHL3 S433C mutant was used as a negative control.

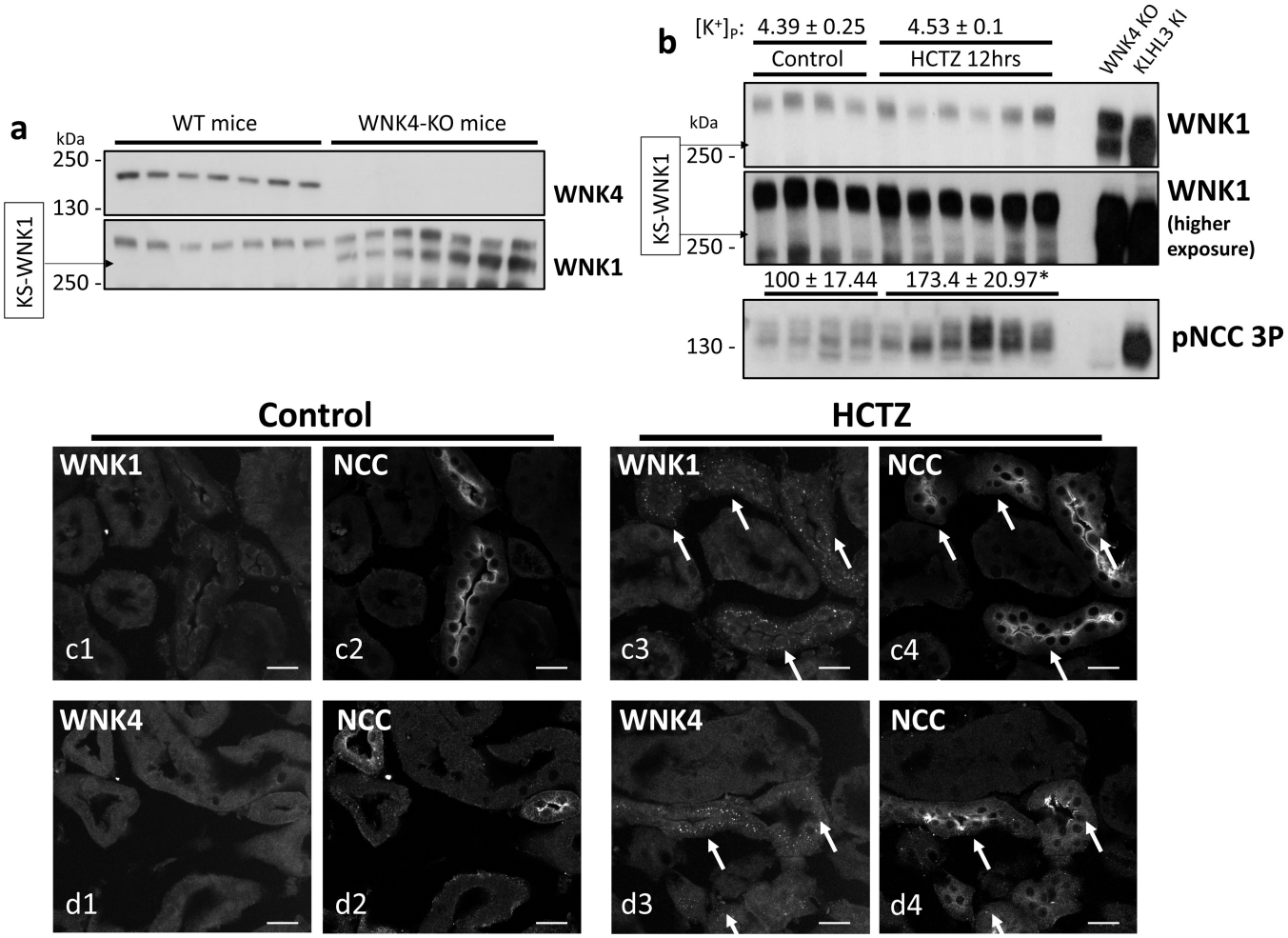

Figure 8.

Increased KS-WNK1 protein levels are observed in WNK4$^{-/-}$ mice and thiazide-treated mice. (A) Immunoblot analysis of kidney proteins from WNK4$^{-/-}$ mice and wild type littermates. The panWNK1 antibody used was previously shown to recognize a band corresponding to KS-WNK1 at the indicated height (black arrow) in immunoblots[49]. (B) Representative immunoblots of kidney proteins from mice treated with vehicle or hydrochlorothiazide (60mg/kg body weight) for 12 hours. Mean plasma [K^+] values for each group are indicated above. (C-D) Immunofluorescent staining of kidney slices from thiazide-treated mice (same animals analyzed in B). Thiazide treatment induces the formation of WNK bodies (detected with the WNK1 and WNK4 antibodies) in DCT cells (NCC positive) (white arrows). Data are mean ± SEM. *p<0.05, **p<0.0001.

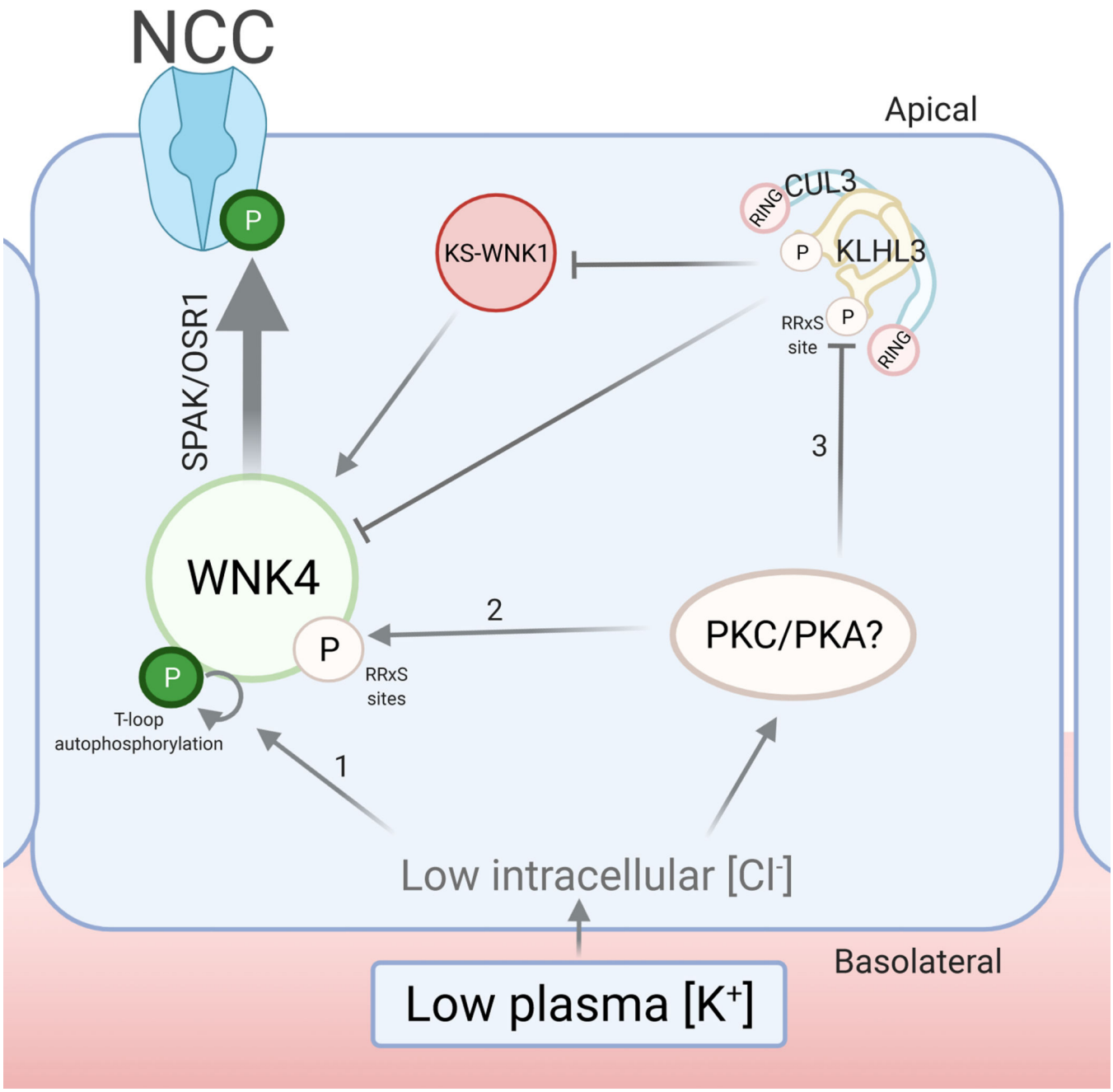

Figure 9.

Proposed model of the mechanisms that contribute to NCC's activation during hypokalemia. With a decrease in plasma [K^+], there is an increase in Cl^- efflux in the basolateral membrane of the DCT. This leads to the activation of WNK4 by three different mechanisms: 1) a reduction in direct Cl^- binding to WNK4 increases its trans-autophosphorylation at its T-loop, 2) the activation of an unknown kinase increases the phosphorylation of WNK4 at its RRxS motifs, also promoting the increase in catalytic activity, and 3) increased inhibitory

KLHL3-S433 phosphorylation decreases KLHL3-targeted degradation of WNKs, leading to increased abundance of WNK4 and KS-WNK1 in the DCT.

Table 1.

Plasma biochemistry of $WNK4^{+/+}$ and $WNK4^{L319F/L319F}$

	$WNK4^{+/+}$	**$WNK4^{L319F/L319F}$**	**p value**
Body weight (g)	27.84 ± 0.57, n=11	27.3 ± 1.13, n=8	0.6524
Plasma [Na^+] (mmol/L)	147.4 ± 0.38, n=13	146.8 ± 0.46, n=9	0.3260
Plasma [K^+] (mmol/L)	4.33 ± 0.08, n=13	4.58 ± 0.11, n=9	0.0738
Plasma [Cl^-] (mmol/L)	120.8 ± 0.9, n=13	121.1 ± 0.95, n=9	0.8451
Plasma [Mg^{2+}] (mg/dL)	1.743 ± 0.02, n=9	1.759 ± 0.06, n=8	0.7947
Plasma [BUN] (mgl/dL)	24.08 ± 0.66, n=12	21 ± 0.85, n=9	0.0088
Plasma [Creatinine] (mg/dL)	0.1082 ± 0.01, n=11	0.0775 ± 0.01, n=8	0.1435
Hematocrit (%)	41.45 ± 0.43, n=11	41.75 ± 0.41, n=8	0.6395
Renin mRNA abundance (% of control)	100.00 ± 10.08, n=8	86.91 ± 8.92, n=5	0.5110
Plasma aldosterone (pg/mL)	455.3 ± 62.16, n=10	361.9 ± 80.38, n=7	0.3656